ISSN 1674-1056
http://cpb.iphy.ac.cn
http://iopscience.iop.org/cpb
中国物理 B
Chinese Physics
中国物理
Chinese Physics B

Laser-driven relativistic electron dynamics in a cylindrical plasma channel

Pan-Fei Geng(耿盼飞), Wen-Juan Lv(吕文娟), Xiao-Liang Li(李晓亮), Rong-An Tang(唐荣安), Ju-Kui Xue(薛具奎)
Citation: Chin. Phys. B . 2018, 27(3): 035201. **doi:** 10.1088/1674-1056/27/3/035201

Journal homepage: http://cpb.iphy.ac.cn; http://iopscience.iop.org/cpb

What follows is a list of articles you may be interested in

Spectral and ion emission features of laser-produced Sn and SnO_2 plasmas

Hui Lan(兰慧), Xin-Bing Wang(王新兵), Du-Luo Zuo(左都罗)
Chin. Phys. B . 2016, 25(3): 035202. **doi:** 10.1088/1674-1056/25/3/035202

Dynamics of laser beams in inhomogeneous electron—positron—ion plasmas

Cheng Li-Hong, Tang Rong-An, Du Hong-E, Xue Ju-Kui
Chin. Phys. B . 2015, 24(7): 075201. **doi:** 10.1088/1674-1056/24/7/075201

High-order optical vortex harmonics generated by relativistic femtosecond laser pulse

Han Yu-Jing, Liao Guo-Qian, Chen Li-Ming, Li Yu-Tong, Wang Wei-Min, Zhang Jie
Chin. Phys. B . 2015, 24(6): 065202. **doi:** 10.1088/1674-1056/24/6/065202

Mitigation of energetic ion debris from Gd plasma using dual laser pulses and the combined effect with ambient gas

Dou Yin-Ping, Sun Chang-Kai, Liu Chao-Zhi, Gao Jian, Hao Zuo-Qiang, Lin Jing-Quan
Chin. Phys. B . 2014, 23(7): 075202. **doi:** 10.1088/1674-1056/23/7/075202

High power terahertz pulses generated in intense laser-plasma interactions

Li Yu-Tong, Wang Wei-Min, Li Chun, Sheng Zheng-Ming
Chin. Phys. B . 2012, 21(9): 095203. **doi:** 10.1088/1674-1056/21/9/095203

Laser-driven relativistic electron dynamics in a cylindrical plasma channel*

Pan-Fei Geng(耿盼飞), Wen-Juan Lv(吕文娟), Xiao-Liang Li(李晓亮), Rong-An Tang(唐荣安), and Ju-Kui Xue(薛具奎)†

Key Laboratory of Atomic & Molecular Physics and Functional Materials of Gansu Province, College of Physics and Electronics Engineering, Northwest Normal University, Lanzhou 730070, China

(Received 8 September 2017; revised manuscript received 12 November 2017; published online 13 February 2018)

The energy and trajectory of the electron, which is irradiated by a high-power laser pulse in a cylindrical plasma channel with a uniform positive charge and a uniform negative current, have been analyzed in terms of a single-electron model of direct laser acceleration. We find that the energy and trajectory of the electron strongly depend on the positive charge density, the negative current density, and the intensity of the laser pulse. The electron can be accelerated significantly only when the positive charge density, the negative current density, and the intensity of the laser pulse are in suitable ranges due to the dephasing rate between the wave and electron motion. Particularly, when their values satisfy a critical condition, the electron can stay in phase with the laser and gain the largest energy from the laser. With the enhancement of the electron energy, strong modulations of the relativistic factor cause a considerable enhancement of the electron transverse oscillations across the channel, which makes the electron trajectory become essentially three-dimensional, even if it is flat at the early stage of the acceleration.

Keywords: laser–plasma interaction, direct laser acceleration, cylindrical plasma channel

PACS: 52.38.–r, 52.38.Kd, 41.75.Jv **DOI:** 10.1088/1674-1056/27/3/035201

1. Introduction

In recent years, laser–plasma interactions have attracted considerable interest.[1–8] Generation of energetic electrons is a key feature of ultra-intense laser–plasma interactions and has been successfully employed in a variety of applications, such as powerful terahertz (THz) radiation,[9–12] particle sources,[13] x-ray and γ-ray emission[14] and ion acceleration.[15–17] Laser-wakefield accelerator,[18–20] the laser beat wave accelerator[21–23] and ponderomotive acceleration[24,25] have been developed in order to enhance the electron energy gain from laser waves and generate high energetic electrons. Electron acceleration with 4.2 GeV energy is being achieved.[26]

Recently, it has been shown that laser-driven relativistic electrons in plasma channels are a potential source of short-wavelength radiation being emitted at the turning points of the electron oscillations in the channel. This emission process is treated in the framework of the direct laser acceleration (DLA) scheme of electrons in plasma channels. This acceleration scheme can be used to explain the high electron energies observed in PIC simulations[27] and in high-intensity laser experiments.[4] In contrast to the laser wakefield acceleration (LWFA),[28] the electrons are directly accelerated by the self-focussed laser field without the presence of a longitudinal wakefield. Direct laser accelerations of electrons in ion channels and plasma bubbles have been considered analytically and through extensive computational work.[29–31]

It is well known that the laser–plasma interaction and thus the mechanism responsible for electron acceleration strongly depend on the duration of laser pulse and the plasma density.[1,32,33] In the case of a long laser beam, its ponderomotive pressure tends to expel plasma electrons from the beam in the transverse direction. This expulsion can be overcome by a plasma channel.[27] Hence, the laser pulse can propagate through the plasma and its propagation is typically accompanied by cavitation of the electron density when the density of plasma is low.[34] It has been shown that a steady-state channel is formed in the plasma in this case with quasi-static transverse and longitudinal electric fields and these relatively weak fields significantly alter the electron dynamics.[35] In addition, it has been shown that parametric instability[36–38] can cause free oscillations of the electron perpendicular to the plane of the driven motion to become unstable.[35,39]

In this paper, the energy and trajectory of the electron in a cylindrical plasma channel with a uniform positive charge and a uniform negative current have been discussed in terms of a single-electron model of direct laser acceleration. We have analyzed the dynamics of the electron which is irradiated by a high-power laser pulse in the channel. We find that the energy and trajectory of the electron strongly depend on the positive charge density, the negative current density, and the intensity

*Project supported by the National Natural Science Foundation of China (Grant Nos. 11475027, 11765017, 11764039, 11305132, and 11274255), the Natural Science Foundation of Gansu Province, China (Grant No. 17JR5RA076), and the Scientific Research Project of Gansu Higher Education, China (Grant No. 2016A-005).

†Corresponding author. E-mail: xuejk@nwnu.edu.cn

© 2018 Chinese Physical Society and IOP Publishing Ltd

of the laser. The electron can be accelerated significantly only when the uniform positive charge density, the uniform negative current density, and the intensity of the laser pulse in suitable ranges. Particularly, when their values satisfy a critical condition, the electron can stay in phase with the laser and gain the largest energy from the laser pulse. Meanwhile, the free oscillations of the electron perpendicular to the plane of the driven motion become unstable due to strong modulations of the relativistic factor associated with the energy enhancement if the electron is initially slightly displaced from the axis of the channel. As a consequence, out of plane displacements grow to become comparable to the amplitude of the driven oscillations and the electron trajectory becomes essentially three-dimensional, even if it is flat at the early stage of the acceleration. Hence, the instability threshold for developing electron acceleration and the electron energy gain from the laser can be controlled by adjusting suitably positive charge density, negative current density, and the intensity of the laser pulse. The free oscillations of the electron perpendicular to the plane of driven motion are likely to become unstable when the electron is accelerated.

2. Model and theoretical analysis

In order to discuss the electron acceleration in a cylindrical plasma channel which is along the x axis with a uniform positive charge density τ and a uniform negative current density j_x, we consider the behavior of a single electron irradiated by a plane electromagnetic wave with frequency ω_0 and intensity I, propagating along the channel with phase velocity $v_{\rm ph} \approx c$. It is convenient to use a Cartesian system of coordinates (x,y,z), with the x axis directed along the axis of the channel and in the direction of the wave propagation. Without any loss of generality, we set the wave electric fields and magnetic fields to be directed along the y and z axes, respectively. Gaussian units are used. The electron is acted by the electric fields $(\boldsymbol{E})$ and magnetic fields $(\boldsymbol{B})$. The electron motion can be described by[37,40]

$$\frac{\mathrm{d}\boldsymbol{p}}{\mathrm{d}t} = -e\boldsymbol{E} - \frac{e}{c}\boldsymbol{v}\times\boldsymbol{B}, \tag{1}$$

where $\boldsymbol{p} = \gamma m_{\rm e}\boldsymbol{v}$ denotes the electron momentum, t denotes the time in the laboratory frame of reference, $m_{\rm e}$ denotes the electron mass, $-e$ denotes the electron charge, $\boldsymbol{v}$ denotes the velocity of the electron, c is the velocity of light and $\gamma = \sqrt{1+p^2/(m_{\rm e}^2c^2)}$ is the relativistic factor. The electric field is a sum of a static field of the space charge $\boldsymbol{E}_{\rm c}$ and an oscillating field of the wave $\boldsymbol{E}_{\rm w}$, that is $\boldsymbol{E} = \boldsymbol{E}_{\rm c} + \boldsymbol{E}_{\rm w}$. $\boldsymbol{E}_{\rm c} = -\boldsymbol{\nabla}\Phi$ and $\boldsymbol{E}_{\rm w} = -(1/c)(\partial\boldsymbol{A}/\partial t)$, respectively. The magnetic field $\boldsymbol{B}$ in Eq. (1) is only due to the wave, $\boldsymbol{B} = \boldsymbol{B}_{\rm w}$, $\boldsymbol{B}_{\rm w} = \boldsymbol{\nabla}\times\boldsymbol{A}$. The electromagnetic fields are derived from the potentials[41]

$$\frac{e\Phi}{m_{\rm e}c^2} = -\frac{1}{2}k_{\rm E}(k_0 r)^2, \tag{2}$$

$$\frac{e\boldsymbol{A}}{m_{\rm e}c^2} = \frac{1}{2}k_{\rm B}(k_0 r)^2 e_x + A_0\sin\xi\, e_y, \tag{3}$$

where $r = \sqrt{y^2+z^2}$ is the electron displacement from the axis of the channel, and $k_0 = \omega_0/c$, $\xi = \omega_0(t-x/c)$. The model includes three dimensionless parameters $k_{\rm E} = \tau/(2en_{\rm c})$, $k_{\rm B} = -j_x/(2en_{\rm c}c)$ and $A_0 = \sqrt{I/I_0}$, being defined in terms of the critical density $n_{\rm c} = m_{\rm e}\omega_0^2/(4\pi e^2)$ and the relativistic unit of laser intensity $I_0 = c(m_{\rm e}\omega_0 c/e)^2/(8\pi)$ with $I_0 = 1.368\times 10^{18}$ W/cm^2 for 1 μm light.

In the following, the variables (x,y,z), p, v, t, E, and B are normalized by c/ω_0, $m_{\rm e}c$, c, $1/\omega_0$, $m_{\rm e}\omega_0 c/e$, and $m_{\rm e}\omega_0/e$, respectively. For simplicity, a new dimensionless parameter τ (normalized by $1/\omega_0$) is used instead of t and defined by the relation $\mathrm{d}t/\mathrm{d}\tau = \gamma$. Hence, $\xi = t - x$ can be derived into the following form:

$$\frac{\mathrm{d}\xi}{\mathrm{d}\tau} = \gamma - p_x, \tag{4}$$

and then, we can obtain the following set of equations for the electron motion:

$$\frac{\mathrm{d}p_x}{\mathrm{d}\xi} = \frac{p_y A_0\cos\xi}{\gamma-p_x} + \frac{k_{\rm B}(yp_y+zp_z)}{\gamma-p_x}, \tag{5}$$

$$\frac{\mathrm{d}p_y}{\mathrm{d}\xi} = A_0\cos\xi - \frac{\gamma k_{\rm E}+k_{\rm B}p_x}{\gamma-p_x}y, \tag{6}$$

$$\frac{\mathrm{d}p_z}{\mathrm{d}\xi} = -\frac{\gamma k_{\rm E}+k_{\rm B}p_x}{\gamma-p_x}z, \tag{7}$$

$$\frac{\mathrm{d}y}{\mathrm{d}\xi} = \frac{p_y}{\gamma-p_x}, \tag{8}$$

$$\frac{\mathrm{d}z}{\mathrm{d}\xi} = \frac{p_z}{\gamma-p_x}. \tag{9}$$

From Eqs. (4), (8), and (9), we have $\mathrm{d}r^2/\mathrm{d}\tau = 2(yp_y + zp_z)$, $\mathrm{d}\sin\xi/\mathrm{d}\tau = (\gamma-p_x)\cos\xi$, and then, by using Eq. (4), equations (5)–(7) become

$$\frac{\mathrm{d}p_x}{\mathrm{d}\tau} = \frac{p_y A_0}{\gamma-p_x}\frac{\mathrm{d}\sin\xi}{\mathrm{d}\tau} + \frac{k_{\rm B}}{2}\frac{\mathrm{d}r^2}{\mathrm{d}\tau}, \tag{10}$$

$$\frac{\mathrm{d}p_y}{\mathrm{d}\tau} = A_0\frac{\mathrm{d}\sin\xi}{\mathrm{d}\tau} - (\gamma k_{\rm E}+k_{\rm B}p_x)y, \tag{11}$$

$$\frac{\mathrm{d}p_z}{\mathrm{d}\tau} = -(\gamma k_{\rm E}+k_{\rm B}p_x)z. \tag{12}$$

It can be derived from the relativistic factor $\gamma = \sqrt{1+p_x^2+p_y^2+p_z^2}$ that

$$\gamma\frac{\mathrm{d}\gamma}{\mathrm{d}\tau} = p_x\frac{\mathrm{d}p_x}{\mathrm{d}\tau} + p_y\frac{\mathrm{d}p_y}{\mathrm{d}\tau} + p_z\frac{\mathrm{d}p_z}{\mathrm{d}\tau}, \tag{13}$$

and then, from Eqs. (10)–(13), we can obtain an important integral of motion

$$\gamma - p_x + \frac{1}{2}(k_{\rm E}+k_{\rm B})r^2 = C, \tag{14}$$

where C is a constant determined by the initial conditions. The dephasing rate $\gamma - p_x$ between the wave and electron motion

can be determined from Eq. (14), which depends on the dimensionless parameters k_E, k_B (which denote the densities of charge and current) and the amplitude of the electron oscillations r across the plasma channel. On the one hand, it sets an upper limit for the amplitude of electron oscillations across the plasma channel. The γ-factor tends to enhance when the amplitude of the electron oscillations across the channel becomes large for some special values of the dimensionless parameters k_E and k_B. On the other hand, the dephasing rate $\gamma - p_x$ between the wave and electron motion limits the electron energy gain from the wave. If the electron moves with laser together, then it can gain more energy from the laser. However, the electron moves slower than the wave and is therefore subject to dephasing. For the same initial displacement, the electron will stay in phase with the wave for a longer time if the dephasing rate $\gamma - p_x$ changes more slowly and $\gamma - p_x$ keeps near zero for a longer time, therefore, the electron can gain more energy from the laser.

Without the charge density and current density (i.e., $k_E = k_B = 0$) and assuming that initially the electron is at rest and its initial displacement from the axis of the channel is small (i.e., $C \approx 1$), equations (11), (12), and (14) indicate that $p_x = (1/2)A_0^2 \sin^2\xi$, $p_y = A_0 \sin\xi$, $p_z = 0$. Then, we can obtain $\gamma = 1 + (1/2)A_0^2 \sin^2\xi$ and its maximum is obviously $\gamma_{vac} = 1 + (1/2)A_0^2$. In order to get the result of $\gamma > \gamma_{vac}$, the dephasing rate $\gamma - p_x$ must be very small. From Eq. (14), we can obtain the dephasing rate as

$$\gamma - p_x \approx 1 - \frac{1}{2}(k_E + k_B)r^2. \tag{15}$$

It can be seen easily from Eq. (15) that the dephasing rate strongly depends on the density of charge, current in the plasma channel, and the amplitude of the electron oscillations across the plasma channel. The dephasing rate $\gamma - p_x \to 0$ only when the values of k_E and k_B satisfy the following relation:

$$k_E + k_B \approx \frac{2}{r_{max}^2}. \tag{16}$$

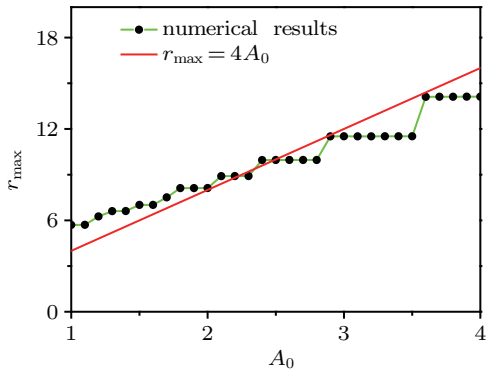


Fig. 1. (color online) The value of r_{max} as a function of A_0 for a series of values of k_E and k_B, the black dots on the line are the numerical results. Obviously, the maximum amplitude of the electron oscillations across the plasma channel r_{max} is proportional to the intensity of the laser A_0: $r_{max} \approx 4A_0$.

From dynamical and kinematical equations of the electron, we can know that the maximum amplitude of the electron oscillations across the plasma channel r_{max} is proportional to the intensity of the laser A_0. In Fig. 1, the numerical results are shown of the value of r_{max} as a function of A_0 for a series of values of k_E and k_B. The green line with the black dots represents the numerical result, the red line satisfies $r_{max} = 4A_0$. As we can see from Fig. 1, those two lines are approximately coincident with each other, hence, we can say that the value of r_{max} is surely proportional to the intensity of the laser A_0 for a series of values of k_E and k_B and the relation of them satisfies $r_{max} \approx 4A_0$. It should be noted that, when the intensity of the laser A_0 becomes large enough, the maximum amplitude of the electron oscillations across the plasma channel r_{max} tends to be saturated for some values of A_0. However, r_{max} increases with A_0 overall. Then, the values of k_E and k_B should be adjusted suitably and the dephasing rate $\gamma - p_x \to 0$ only when the values of them satisfy the following relation:

$$k_E + k_B \approx \frac{1}{8A_0^2}. \tag{17}$$

The electron can be accelerated obviously with the result of $\gamma > \gamma_{vac}$ at this moment. Hence, there is a maximum value area of $\gamma_{max}/\gamma_{vac}$ in (k_E, k_B) space where $k_E + k_B \approx 1/(8A_0^2)$ is satisfied. In addition, equation (16) indicates that the value of r_{max} becomes large with the decrease of k_E, k_B when the electron is accelerated, so, the dephasing rate $\gamma - p_x$ keeps near zero for longer time and the electron can gain more energy from the wave. Hence, we conclude that the electron energy gain from the wave strongly depends on the values of k_E, k_B and A_0. For the fixed value of A_0, the electron can be accelerated significantly and gain more energy from the laser only when $k_E + k_B \approx 1/(8A_0^2)$. The variation of the maximum amplitude of the electron oscillations across the plasma channel r_{max} and the electron maximum energy gain from the wave γ_{max} against the value of dimensionless parameters k_E, k_B and A_0 have similar characters. The electron trajectory may change from planar two-dimensional motion to three-dimensional motion when the electron is accelerated significantly and gain more energy from the laser due to strong modulations of the relativistic γ-factor. Therefore, the instability threshold for developing electron acceleration and the electron energy gain can be controlled by adjusting suitably the values of k_E, k_B and A_0. The numerical results confirm these predictions.

3. Numerical results

To confirm the theoretical prediction, we solve Eqs. (4)–(9) numerically when the initial conditions are given. We use the initial conditions of $x(0) = 0$, $y(0) = 0.01$, $z(0) = 0.05$, $p_x(0) = p_y(0) = p_z(0) = 0$ in all cases.

Figure 2 shows $\gamma_{max}/\gamma_{vac}$, r_{max}, $|z|_{max}/|y|_{max}$ as a function of k_E, k_B, and A_0, respectively. $\gamma_{max}/\gamma_{vac} > 1$ indicates

that the electron can be accelerated significantly and gain more energy from the wave. The value of $r_{\max}$ represents the maximum amplitude of electron oscillations across the plasma channel. The $|z|_{\max}/|y|_{\max} \ll 1$ indicates that the electron trajectory is a stable planar two-dimensional motion, while $|z|_{\max}/|y|_{\max} \sim 1$ indicates that the electron trajectory is unstable and three-dimensional motion occurs. From Fig. 2, we can easily find that the developing of instability and the electron energy gain strongly depend on three parameters $k_{\rm E}$, $k_{\rm B}$, and A_0. For the fixed value of A_0, as we can see obviously from Figs. 2(a)–2(c), the electron energy is very low ($\gamma_{\max}/\gamma_{\rm vac} < 1$) when the values of $k_{\rm E}$ and $k_{\rm B}$ are far below the line of $k_{\rm E}+k_{\rm B} \approx 1/(8A_0^2)$, which is marked by a red line in Fig. 2, it indicates that the electron gets litter energy from the wave and cannot be accelerated in these ranges. In this case, as we can see from Figs. 2(d)–2(i), the corresponding value of $r_{\max}$ is also very small and the electron trajectory is a stable planar two-dimensional motion due to the low energy of the electron. However, there is a maximum value area of $\gamma_{\max}/\gamma_{\rm vac}$ where equation (17) is approximately satisfied, it indicates that the electron can stay in phase with the wave for a longer time and gain more energy from the wave. In the meantime, the corresponding value of $r_{\max}$ is also maximum and the electron trajectory begins to become instable and tends to become a three-dimensional motion due to strong modulations of the relativistic γ-factor associated with the energy enhancement when the values of $k_{\rm E}$ and $k_{\rm B}$ approximately satisfy $k_{\rm E}+k_{\rm B} \approx 1/(8A_0^2)$. Finally, the electron energy tends to decrease gradually with the increase of the values of $k_{\rm E}$, $k_{\rm B}$ when the values of $k_{\rm E}$ and $k_{\rm B}$ are far beyond the line of $k_{\rm E}+k_{\rm B} \approx 1/(8A_0^2)$, i.e., $k_{\rm E}+k_{\rm B} > 1/(8A_0^2)$. The maximum value area of $\gamma_{\max}/\gamma_{\rm vac}$ (indicated by the line of $k_{\rm E}+k_{\rm B} \approx 1/(8A_0^2)$) shrinks to small values of $(k_{\rm E}, k_{\rm B})$ region with the increase of A_0. As we can see from Figs. 2(g)–2(i), the electron trajectory becomes unstable and the possibility that the electron trajectory becomes a three-dimensional motion from a stable planar two-dimensional motion increases when $k_{\rm E}+k_{\rm B} > 1/(8A_0^2)$. This is particularly significant when A_0 is larger.

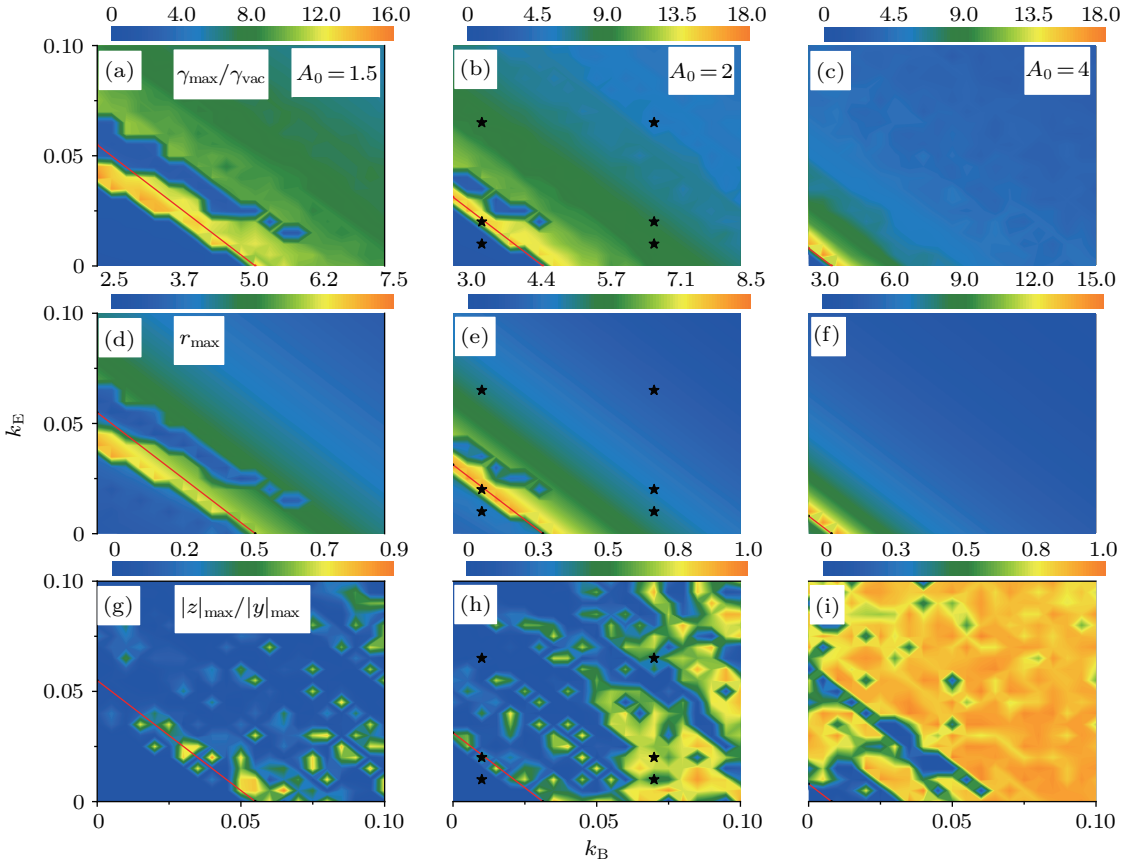


Fig. 2. (color online) $\gamma_{\max}/\gamma_{\rm vac}$ ((a)–(c)), $r_{\max}$ ((d)–(f)), and $|z|_{\max}/|y|_{\max}$ ((g)–(i)) as a function of $k_{\rm E}$, $k_{\rm B}$, and A_0, respectively. The red line is given by Eq. (17).

These conclusions demonstrate our theoretical predictions from the integral of motion. We can see that the electron can gain the largest energy only when the values of $k_{\rm E}$, $k_{\rm B}$, and A_0 are in a suitable range, i.e., equation (17) is approximately satisfied. Hence, the instability threshold for developing electron acceleration and the electron energy gain can be controlled by adjusting suitably the values of $k_{\rm E}$, $k_{\rm B}$, and A_0. However, with the enhancement of the electron energy, strong

modulations of the relativistic factor cause a considerable enhancement of the electron transverse oscillations across the channel, which makes the electron trajectory become a three-dimensional motion.

Figure 3 shows the electron energy $\gamma/\gamma_{\rm vac}$ and the dephasing rate $\gamma - p_x$ as a function of the axial distance x travelled by the electron in a uniform plasma channel for different values of positive charge density $k_{\rm E}$ and negative current density $k_{\rm B}$, the values of $k_{\rm E}$ and $k_{\rm B}$ are marked by a black pentagram in Fig. 2(b). $\gamma/\gamma_{\rm vac} > 1$ and the period of $\gamma/\gamma_{\rm vac}$ becomes large indicating that the electron can be accelerated significantly and gain more energy from the wave. The dephasing rate $\gamma - p_x$ changes more slowly and keeps near zero for a longer time indicating that the electron can stay in phase with the wave for a longer time and gain more energy from the wave. From Fig. 3, we can easily find that the values of $\gamma/\gamma_{\rm vac}$ and $\gamma - p_x$ strongly depend on the values of $k_{\rm E}$ and $k_{\rm B}$. As we can see from Fig. 3, both the energy and acceleration period of the electron are very small and the dephasing rate $\gamma - p_x$ changes very quickly and keeps near 1 for a longer time when the values of $k_{\rm E}$ and $k_{\rm B}$ are far below the line of $k_{\rm E} + k_{\rm B} \approx 1/(8A_0^2)$ ($k_{\rm E} = 0.01$, $k_{\rm B} = 0.01$) in Fig. 2(b), which indicates that the electron gets less energy from the wave and cannot be accelerated in this case. However, both the energy and acceleration period of the electron enhance obviously and the dephasing rate $\gamma - p_x$ changes very slowly and keeps near zero for longer time when the values of $k_{\rm E}$ and $k_{\rm B}$ satisfy Eq. (17), which indicates that the electron gets larger energy from the wave and can be accelerated significantly in this case. The electron energy decreases when the values of $k_{\rm E}$ and $k_{\rm B}$ are far beyond the line of $k_{\rm E} + k_{\rm B} \approx 1/(8A_0^2)$ ($k_{\rm E} = 0.05$, $k_{\rm B} = 0.01$) in Fig. 2(b). In addition, we can also find that the maximum value of $\gamma/\gamma_{\rm vac}$ and the acceleration period of the electron tend to increase with the decrease of the values of $k_{\rm E}$ and $k_{\rm B}$ when the electron is accelerated. At the meanwhile, the dephasing rate $\gamma - p_x$ changes more slowly and keeps near zero for longer time with the decrease of the values of $k_{\rm E}$ and $k_{\rm B}$. These conclusions are consistent with the former discussion about the integral of motion and the information in Fig. 2(b). Hence, the electron energy gain from the laser wave can be controlled by adjusting suitably the values of $k_{\rm E}$, $k_{\rm B}$, and A_0.

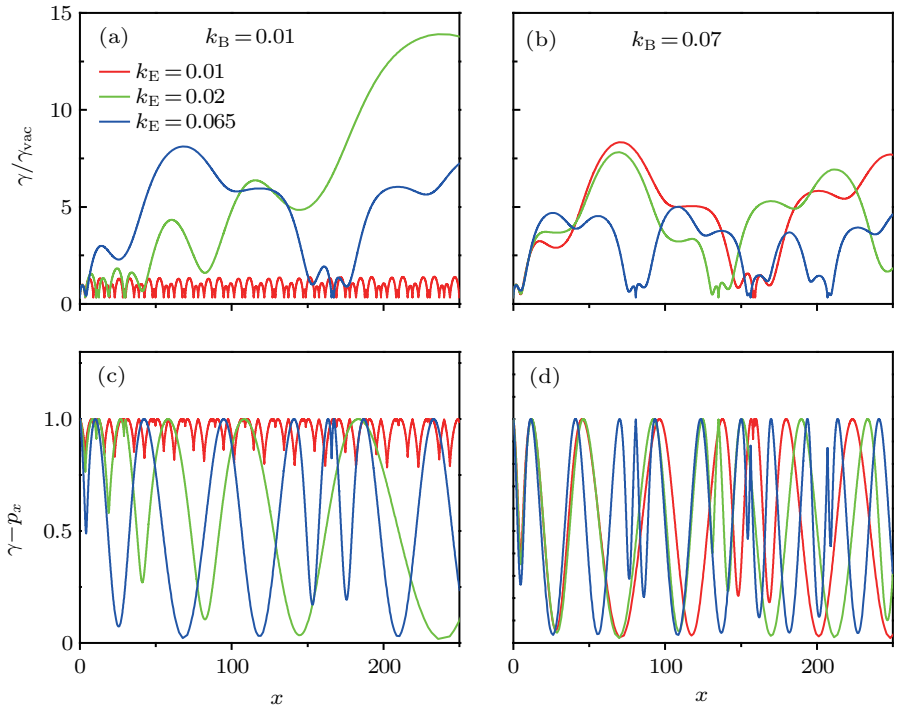


Fig. 3. (color online) The γ-factor ((a) and (b)) and the dephasing rate $\gamma - p_x$ ((c) and (d)) as a function of the axial distance travelled by the electron in a uniform plasma channel for different values of positive charge density and negative current density. The values of $k_{\rm E}$ and $k_{\rm B}$ are marked by a black pentagram in Fig. 2(b). We set $A_0 = 2$ in all cases.

Figure 4 shows that the electron trajectories change with the values of $k_{\rm E}$ and $k_{\rm B}$ when A_0 is fixed ($A_0 = 2$), which corresponds to Fig. 2(h). From Fig. 4(a), we can easily find that the electron trajectory is a stable planar two-dimensional motion and the distance that the electron moves with the laser is very short when the values of $k_{\rm E}$ and $k_{\rm B}$ are far below the line of $k_{\rm E} + k_{\rm B} \approx 1/(8A_0^2)$ ($k_{\rm E} = 0.01$, $k_{\rm B} = 0.01$) in Fig. 2(h). Figures 4(b)–4(f) indicate that the electron trajectory begins to become unstable slightly due to strong modulations of relativistic γ-factor and the distance that the electron moves with the laser enhances obviously when the electron is accelerated (the values of $k_{\rm E}$ and $k_{\rm B}$ satisfy $k_{\rm E} + k_{\rm B} > 1/(8A_0^2)$). We conclude that

the electron trajectory can be a stable planar two-dimensional motion due to the low energy of the electron when the electron is not accelerated, but the free oscillations of the electron perpendicular to the plane of driven motion are likely to become unstable due to strong modulations of relativistic γ-factor associated with the energy enhancement when the electron is accelerated. As a consequence, out of plane displacements grow to become comparable to the amplitude of the driven oscillations and the electron trajectory becomes essentially three-dimensional, even if it is flat at the early stage of acceleration.

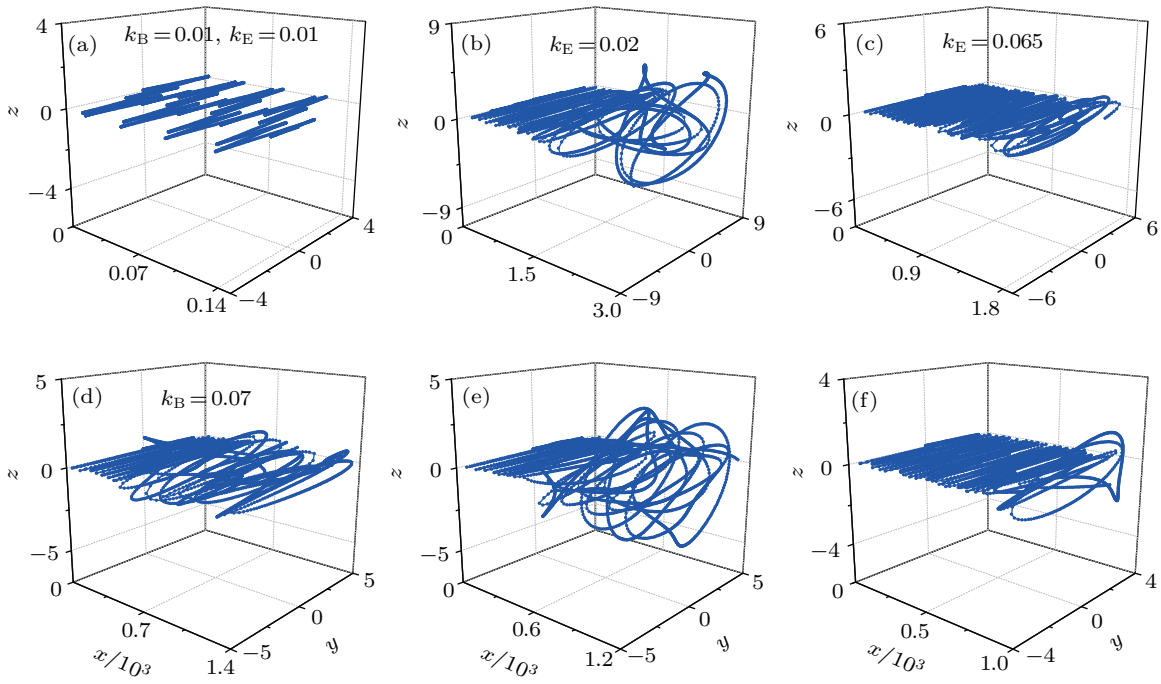


Fig. 4. (color online) The electron trajectories in a cylindrical plasma channel for different values of negative current density (k_B=0.01 for (a)–(c) and k_B=0.07 for (d)–(f)) and positive charge density k_E. We set $A_0 = 2$ in all cases.

4. Summary

In conclusion, the energy and trajectory of the electron, which is irradiated by a high-power laser pulse in a cylindrical plasma channel with a uniform positive charge and a uniform negative current, have been discussed in terms of a single-electron model of direct laser acceleration. We find that the energy and trajectory of the electron strongly depend on the positive charge density, the negative current density, and the intensity of the laser pulse. The electron can be accelerated significantly only when the uniform positive charge density, the uniform negative current density, and the intensity of the laser pulse in suitable ranges due to the dephasing rate between the wave and electron motion. Particularly, when the values of them satisfy a critical condition, the electron can stay in phase with the laser and gain the largest energy from the laser. Hence, the instability threshold for developing electron acceleration and the electron energy gain from the laser can be controlled by adjusting suitably positive charge density, negative current density and the intensity of the laser pulse. Besides, we also show that strong modulations of the relativistic factor cause a considerable enhancement of the electron transverse oscillations across the channel when the electron is accelerated, which makes the electron trajectory become essentially three-dimensional, even if it is flat at the early stage of the acceleration.

References

[1] Esarey E, Schroeder C B and Leemans W P 2009 *Rev. Mod. Phys.* **81** 1229
[2] Leemans W and Esarey E 2009 *Phys. Today* **62** 44
[3] Hooker S M 2013 *Nat. Photonics* **7** 775
[4] Gahn C, Tsakiris G D, Pukhov A, Meyer-ter-Vehn J, Pretzler G, Thirolf P, Habs D and Witte K J 1999 *Phys. Rev. Lett.* **83** 4772
[5] Leemans W P, Catravas P, Esarey E, Geddes C G R, Toth C, Trines R, Schroeder C B, Shadwick B A, Tilborg J and Faure J 2002 *Phys. Rev. Lett.* **89** 174802
[6] Ting A, Moore C I, Krushelnick K, Manka C, Esarey E, Sprangle P, Hubbard R, Burris H R, Fischer R and Baine M 1997 *Phys. Plasma* **4** 1889
[7] Goloviznin V V and Shep T J 1999 *JETP Lett.* **70** 450
[8] Shen B and Yu M Y 2002 *Phys. Rev. Lett.* **89** 275004
[9] Liao G Q, Li Y T, Li C, Su L N, Zheng Y, Liu M, Wang W M, Hu Z D, Yan W C, Dunn J, Nilsen J, Hunter J, Liu Y, Wang X, Chen L M, Ma J L, Lu X, Jin Z, Kodama R, Sheng Z M and Zhang J 2015 *Phys. Rev. Lett.* **114** 255001
[10] Li Y T 2012 *Appl. Phys. Lett.* **100** 254101
[11] Zhuo H B, Zhang S J, Li X H, Zhou H Y, Li X Z, Zou D B, Yu M Y, Wu H C, Sheng Z M and Zhou C T 2017 *Phys. Rev. E* **95** 013201
[12] Zhou M L, Liu F, Li C, Du F, Li Y T, Wang W M, Sheng Z M, Chen L M, Ma J L, Lu X, Dong Q L and Zhang J 2012 *Chin. Phys. Lett.* **29** 015202
[13] Pomerantz I, McCary E, Meadows A, Arefiev A, Bernstein A, Chester C, Cortez J, Donovan M, Dyer G, Gaul E, Hamilton D, Kuk D, Lestrade A, Wang C, Ditmire T and Hegelich B 2014 *Phys. Rev. Lett.* **113** 184801

[14] Ledingham K W D, Spencer I, McCanny T, Singhal R P, Santala M I K, Clark E, Watts I, Beg F N, Zepf M, Krushelnick K, Tatarakis M, Dangor A E, Norreys P A, Allott R, Neely D, Clark R J, Machacek A C, Wark J S, Cresswell A J, Sanderson D C W and Magill J 2000 *Phys. Rev. Lett.* **84** 899

[15] Clark E L, Krushelnick K, Davies J R, Zepf M, Tatarakis M, Beg F N, Machacek A, Norreys P A, Santala M I K, Watts I and Dangor A E 2000 *Phys. Rev. Lett.* **84** 670

[16] Mackinnon A J, Sentoku Y, Patel P K, Price D W, Hatchett S, Key M H, Andersen C, Snavely R and Freeman R R 2002 *Phys. Rev. Lett.* **88** 215006

[17] Xu M H, Li Y T, Liu F, Zhang Y, Lin X X, Wang S J, Meng L M, Wang Z H, Zheng J, Sheng Z M, Wei Z Y, Li Y J and Zhang J 2011 *Acta Phys. Sin.* **60** 045204 (in Chinese)

[18] Tajima T and Dawson J M 1979 *Phys. Rev. Lett.* **43** 267

[19] Sprangle P, Esarey E, Ting A and Joyce G 1988 *Appl. Phys. Lett.* **53** 2146

[20] Wittig G, Karger O, Knetsch A, Xi Y, Deng A, Rosenzweig J B, Bruhwiler D L, Smith J, Manahan G G, Sheng Z M, Jaroszynski D A and Hidding B 2015 *Phys. Rev. Stab.* **18** 081304

[21] Rosenzweig M N and Liu C S 1972 *Phys. Rev. Lett.* **29** 701

[22] Joshi C, Mori W B, Katsouleas T, Dawson J M, Kindel J M and Forslund D W 1984 *Nature* **311** 525

[23] Kitagawa Y, Matsumoto T, Minamihata T, Sawai K, Matsuo K, Mima K, Nishihara K, Azechi H, Tanaka K A, Takabe H and Nakai S 1992 *Phys. Rev. Lett.* **68** 48

[24] Kawata S, Kong Q, Miyazaki S, Miyauchi K, Sonobe R, Sakai K, Nakajima K, Masuda S, Ho Y K, Miyanaga N, Limpouch J and Andrew A A 2005 *Laser Part. Beams* **23** 61

[25] Andreev A, Platonov K and Kawata S 2009 *Laser Part. Beams* **27** 449

[26] Leemans W P, Gonsalves A J, Mao H S, Nakamura K, Benedetti C, Schroeder C B, Tóth Cs, Daniels J, Mittelberger D E, Bulanov S S, Vay J L, Geddes C G R and Esarey E 2014 *Phys. Rev. Lett.* **113** 245002

[27] Pukhov A, Sheng Z M and Meyer-ter-Vehn J 1999 *Phys. Plasmas* **6** 2847

[28] Esarey E, Schroeder C B, Leemans W P and Hafizi B 1999 *Phys. Plasmas* **6** 2262

[29] Zhang X, Khudik V N and Shvets G 2015 *Phys. Rev. Lett.* **114** 184801

[30] Zhang X, Khudik V N, Pukhov A and Shvets G 2016 *Plasma Phys. Control. Fusion* **58** 034011

[31] Shaw J L, Tsung F S, Vafaei-Najafabadi N, Marsh K A, Lemos N, Mori W B and Joshi C 2014 *Plasma Phys. Control. Fusion* **56** 084006

[32] Kemp A J and Divol L 2012 *Phys. Rev. Lett.* **109** 195005

[33] Zhang R, Cheng L H, Tang R A and Xue J K 2016 *Phys. Plasmas* **23** 093105

[34] Sentoku Y, Kruer W, Matsuoka M and Pukhov A 2006 *Fusion Sci. Technol.* **49** 278

[35] Arefiev A V, Khudik V N, Robinson A P L, Shvets G, Willingale L and Schollmeier M 2016 *Phys. Plasmas* **23** 056704

[36] Khudik V N, Arefiev A V, Zhang X and Shvets G 2016 *Phys. Plasmas* **23** 103108

[37] Arefiev A V, Breizman B N, Schollmeier M and Khudik V N 2012 *Phys. Rev. Lett.* **108** 145004

[38] Arefiev A V, Khudik V N and Schollmeier M 2014 *Phys. Plasmas* **21** 033104

[39] Arefiev A V, Khudik V N, Robinson A P L, Shvets G and Willingale L 2016 *Phys. Plasmas* **23** 023111

[40] Arefiev A V, Khudik V N and Schollmeier M 2014 *Phys. Plasmas* **21** 033104

[41] Schmitz M and Kull H J 2002 *Europhys. Lett.* **58** 382